DOI 10.1007/s11182-024-03162-9
Russian Physics Journal, Vol. 67, No. 5, May, 2024

PLASMA PHYSICS

CATHODE PLASMA EXPANSION AT EARLY VACUUM ARC AT PULSED PLASMA EMISSION

A. V. Kozyrev, V. Yu. Kozhevnikov, and A. O. Kokovin UDC 537.533

The paper focuses on the kinetic modeling of the vacuum arc initiation at the pulse-periodic plasma emission from the cathode surface. A comparative analysis is given to the pulse-periodic and continuous plasma emission from the cathode. An in-depth study concerns the mechanism of the anomalous acceleration of ions and cathode plasma expansion at a short-time emission current switch over, matching the plasma emission and its interruption.

Keywords: vacuum discharge, collision-free plasma, ectons, Vlasov equation, virtual cathode.

INTRODUCTION

For several decades, the problem of electrotransmission through the plasma under the vacuum arc conditions is still relevant. These studies involve physical phenomena and processes which cover different spatial and temporal scales. One of such phenomena is the electron beam generation in a vacuum diode with a plasma cathode due to the explosive electron emission or laser initiation. This phenomenon is widely used in high-current electronics, for example, in ion sources [1].

According to the ecton model of the vacuum arc discharge, the cathode plasma (or cathode flare plasma) formation results from the explosion of microscopic irregularities on the cathode surface [1]. Based on the available experiments, it is known that the cathode plasma expands into the discharge gap at velocities significantly higher than the expected values of the substance evaporation [2]. Average ion velocities in vacuum arcs correspond to kinetic energies of tens and even hundreds of electron volts, while thermal energies of plasma particles are usually limited to units of electron volts. Since kinetic energies of these ions are much higher than the arc discharge voltage (usually 80 V or less), such ions can be characterized as possessing anomalously high energies. A transfer of such ions in vacuum arcs, is called anomalous acceleration of positively charged ions emitting from the cathode region with the low current potential to the anode with the high current potential [1]. Earlier Oks *et al.* [3] prove that up to 10–12% of the total electric charge passing through the collector (anode) in vacuum arc discharges belongs to the anomalous ion transfer.

From the theoretical point of view, the anomalous ion acceleration is a serious problem requiring the appropriate quantitative description in terms of an internally non-contradictory theory. According to [2], theoretical hypotheses of the ion flux directed to the anode, can be divided into three physically distinct groups: explosive, collision, and electrodynamic.

The explosive mechanism hypothesis [4] is based on the assumption that the cathode plasma results from a continuous transition of matter from the solid state to the ideal cathode flare plasma through intermediate states of liquid metal, metal vapor and non-ideal plasma. Very large spatial gradients of the matter particle concentration resulting from this phase transition, provide anode-oriented ion fluxes with the velocities observed.

Institute of High Current Electronics of the Siberian Branch of the Russian Academy of Sciences, Tomsk, Russia, e-mail: kozyrev@to.hcei.tsc.ru; v.y.kozhevnikov@yandex.ru; kokovin@to.hcei.tsc.ru. Original article submitted March 19, 2024.

The collision mechanism hypothesis, e.g., [5, 6], implies that the cathode flare plasma is dense enough to support the intensive interaction between the electron and ion flow and between ionic species. It is assumed that elastic collisions between electrons and ions, facilitate an electron-to-ion mechanical energy transfer, leading to their accelerated flow toward the anode. This process is figuratively called the electron-wind effect.

The hypothesis of electrodynamic mechanism assumes, that the cathode plasma expansion is provided by the formation of a non-monotonic distribution of the current potential near the cathode (potential hump theory) [7]. The electric field effect causes the accelerated ion motion from the cathode to the anode, providing the dynamics of doubly and triply charged ions (M++, M+++), which may be present in the cathode spot plasma of a number of materials [8]. Serious arguments in favor of this hypothesis are given in the monograph by Mesyats [1], who presents comprehensive experimental results of the anomalous expansion of the cathode plasma.

In the years 2021–2023, a consistent collision-free kinetic theory of the cathode plasma expansion was formulated in theoretical works [9–13] of researchers from the Institute of High-Current Electronics of the Siberian Branch of the Russian Academy of Sciences. It not only explained in detail the physical nature of the phenomenon, but also predicted the expansion rate in vacuum diodes of different configuration. It was shown that during the vacuum arc formation, the collision-free electric field was the key physical mechanism of the cathode plasma expansion. It implied that the peripheral region of the dense cathode plasma in the external electric field acquired an excessive negative bulk charge resulting in the formation of a virtual cathode $\Delta\varphi < 0$. The potential drop affected accelerating forces acting on the ions at the plasma emission centre, that made ions to move to the anode and acquire anomalously high values of the kinetic energy, *viz*. $\varepsilon_i > qU_0$. This effect was determined by the emission centre parameters, rather than the voltage U_0 applied to the diode. Moreover, that theory explained why the potential hump could not detected experimentally [14]: the region of the acceleration potential drop was very thin.

Conclusions in works [9–13] were based on the important assumption that the cathode plasma emission occurred in a continuous mode. As noted in [1], the electron flow of the explosive electron emission arrived in the form of bursts. These bursts of plasma emitted from the explosive emission centres, were conventionally associated with emission quasiparticles called ectons [1]. The idea of ectons arose from observations of vacuum sparks and arcs, as the processes at the explosive emission centres were mostly cyclic [15], i.e., the plasma emission appeared, continued for a certain time, interrupted, and then started again. Electron-optical observations indicated a discontinuous glow at the emission centre. For example, Cross *et al*. [16] reported that the glow appeared and disappeared at least five times during several tens of nanoseconds. For the copper cathode, the glow was observed at a 5 ns cycle and 3 to 5 ns lifetime of the emission centre [17].

The aim of this work is to study the probable ecton mechanism during the anomalous acceleration of ions and cathode plasma expansion. In terms of the kinetic approach formulated earlier [8, 9], the cathode plasma emission is clarified, and the numerical solution of kinetic equations for a planar vacuum diode is discussed with regard to the periodic changes in the emission current density. The proposed approach clearly shows that the early identified collision-free mechanism is still relevant for the pulsed plasma emission.

THEORETICAL MODEL OF PLANAR VACUUM DIODE WITH EXPLOSIVE EMISSION

The mathematical model described in more detail in [10], was used in our calculations. Let us consider a plane vacuum diode formed by the vacuum gap of the length D with the cross-sectional area S. The electron and ion distribution functions are parameterized by three independent variables: the Cartesian coordinate x, collinear pulse component p_x, and time t. These parametrized functions also obey the collision-free, non-relativistic kinetic equations:

$$\begin{cases} \dfrac{\partial f_e}{\partial t} + \dfrac{p_x}{m_e}\dfrac{\partial f_e}{\partial x} - qE_x\dfrac{\partial f_e}{\partial p_x} = 0, \\ \dfrac{\partial f_i^+}{\partial t} + \dfrac{p_x}{m_i}\dfrac{\partial f_i^+}{\partial x} + qE_x\dfrac{\partial f_i^+}{\partial p_x} = 0, \end{cases} \tag{1}$$

where q is the electron charge, E_x is the electric field intensity along the coordinate axis x; m_e and m_i are electron and ion rest masses, respectively.

According to Kozhevnikov *et al*. [9], the model is collision-free; the right-hand side of Eq. (1) does not contain integrals of elastic and/or inelastic collisions. For simplicity, let us assume that the cathode plasma consists only of electrons and single-charged ions of one species, which is a reasonable assumption for cathodes made of lithium, carbon, bismuth, and some other materials [8]. In calculations below, it is assumed that the cathode material is antimony Sb (m_i = 121 amu), for which the two-component plasma is relevant.

By analogy with the work [9], the system of kinetic equations (1) is added by Poisson's equation to calculate the electrostatic potential φ and the electric field E_x of the vacuum diode, both controlled by the dynamics of the bulk charge of ions and electrons:

$$\frac{\partial^2 \varphi}{\partial x^2} = -\frac{q}{\varepsilon_0}\left(n_+ - n_e\right), \quad E_x = -\frac{\partial \varphi}{\partial x}, \tag{2}$$

where ε_0 is the vacuum permeability, n_+ is the ion concentration, n_e is the electron concentration.

Ion and electron concentrations are determined as zero-moment electron distribution and ion distribution functions using a standard technique:

$$n_e(x,t) = \int_{-\infty}^{\infty} f_e(x,p_x,t)\,dp_x, \quad n_+(x,t) = \int_{-\infty}^{\infty} f_i^+(x,p_x,t)\,dp_x\,. \tag{3}$$

In order to describe the delay stage of the vacuum arc, let us consider the vacuum diode in the circuit of the voltage supply $U(t)$ with the ballast resistor R connected in series. The simplicity of the electrical circuit of the planar vacuum diode allows us to write Poisson's equation (2) as analytical, using the quadrature formulas:

$$\begin{aligned} E_x(x,t) &= -\frac{U(t)-j(t)SR}{D} + \frac{q}{\varepsilon_0 D}\int_0^D\int_0^x \left[n_e(x',t)-n_i(x',t)\right]dx'dx - \frac{q}{\varepsilon_0}\int_0^x \left[n_e(x',t)-n_i(x',t)\right]dx', \\ \varphi(x,t) &= \left\{U(t)-j(t)SR - \frac{q}{\varepsilon_0}\int_0^D\int_0^x \left[n_e(x',t)-n_i(x',t)\right]dx'dx\right\}\frac{x}{D} + \frac{q}{\varepsilon_0}\int_0^x\int_0^{x'} \left[n_e(x'',t)-n_i(x'',t)\right]dx''dx', \end{aligned} \tag{4}$$

where $j(t)$ is the current density with uniform gap length, which is determined by a sum of convection current density of charged particles $j_e(x, t)$ and $j_i(x, t)$ and displacement current density:

$$\begin{aligned} &\varepsilon_0 \frac{\partial E_x}{\partial t} + j_i - j_e = j(t), \\ &j_e(x,t) = q\int_{-\infty}^{\infty} \frac{p_x}{m_e} f_e(x,p_x,t)\,dp_x, \quad j_i(x,t) = q\int_{-\infty}^{\infty} \frac{p_x}{m_i} f_i^+(x,p_x,t)\,dp_x. \end{aligned} \tag{5}$$

Analogously to the basic concepts by Kozhevnikov *et al*. [9], we assume that the vacuum gap is empty at zero-moment t = 0, which is expressed by the following conditions:

$$f_e(t=0) = f_i^+(t=0) \equiv 0\,. \tag{6}$$

However, in contrast to the boundary conditions for the continuous emission [9], the following boundary conditions for electron/ion distribution functions are used for the ecton model of nonstationary processes:

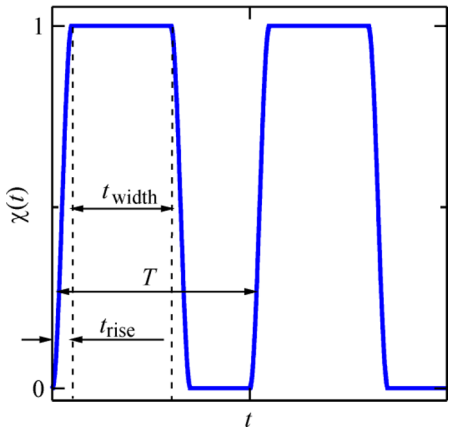

Fig. 1. Time dependence between cathode plasma concentration in ectons: t_{rise} – rising/falling edge duration, t_{width} – signal length, T – signal cycle.

$$f_e\left(x=0,p_x,t\right)=\frac{n_0\chi(t)}{\sqrt{2\pi m_e T_e}}e^{-\frac{p_x^2}{2m_eT_e}},\quad f_i^+\left(x=0,p_x,t\right)=\frac{n_o\chi(t)}{\sqrt{2\pi m_i T_i}}e^{-\frac{p_x^2}{2m_iT_i}},\tag{7}$$

where T_e and T_i are kinetic temperatures of respectively electrons and ions of the cathode plasma, approaching to the explosive electron emission parameters $T_e \sim 5$ eV and $T_i \sim 1$ eV [1], n_0 is the quasi-neutral plasma at the emission centre, $\chi(t)$ is the function of the unit impulse signal, describing nonstationary emission shown in Fig. 1.

The system of equations (1) with the initial (6) and boundary (7) conditions and the electric field from Eq. (4), is solved by using a grid method applied to a quasi-uniform rectangular grid of the phase space (N_x, N_{px}), where N_x and N_{px} are numbers of sections of mesh spacing by coordinates x and p_x, respectively. Depending on the numerical result extension, the spacing parameters are varied in wide ranges, namely $N_x = 1000$ to 3000 and $N_{px} = 1000$ to 2000.

Mesh spacing by pulses p_x is uniform, with the enough maximum value of electron and ion momenta, while mesh spacing by the coordinate is three-layer quasi-uniform:

$$x(\xi)=\frac{D}{2}+\frac{c\xi}{\sqrt{1+d\xi^2}},\quad \xi\in[-1,1],$$

where ξ is the uniform grid parameter in the interval [–1, 1]. Parameters c and d were used for the gap $D = 1$ cm, in order for the computational cell size near the cathode to be 10 to 15 times smaller than the Debye length $L_D=\sqrt{\varepsilon_0 W_e / q^2 n_0}$.

The general scheme of the numerical algorithm coincided with that used in the work [9]. The semi-Lagrangian scheme [18] with higher-order cubic spline interpolation [19] and additionally modified Akima interpolation methods [20] were used to solve the Vlasov equations in the specified mesh spacing. The computational algorithm was implemented as the GNU C programming language with OpenMP and GNU Scientific Libraries. MATLAB (MathWorks) interactive environment for numerical computation, visualization and programming was used for processing the data obtained.

Cathode plasma expansion and continuous emission

The model of switching the external source with $U(t)$ voltage with the rising edge $t_{rise} = 0.1$ ns and $U_0 = 2$ kV *via* the ballast resistor R was created to study the vacuum arc in the planar gap. The electrode gap was $D = 1$ cm. The

product of the ballast resistor R by the cross-sectional area S was 200 Ω·cm^2. The boundary condition of the plasma emission represented the pulse-periodic function with the basis plasma concentration $n_0 = 10^{22}$ m^{-3}.

Figure 2 illustrates the cathode plasma expansion at its continuous emission $\chi(t) = 1$. This mechanism is studied in detail in [9]. At the start time (1 or 2 ns), after the anode voltage application, electrons accelerate due to the external field, and the electron charge relaxation occurs inside the diode, that ends in the electron flow in accordance with the Child-Langmuir law. Electrons arrived at the anode, acquire the average kinetic energy equaling to the anode voltage multiplied by the electron charge, *viz*. $\varepsilon_e = qU_0$.

The motion of part of electrons emitted onto the anode, leads to the formation of the current potential Δφ lower than the cathode potential, with the depth of several tens of volts at the periphery of the cathode plasma bunch (virtual cathode). The electric force, which causes a non-thermal ion motion towards the anode, initiates between the physical and virtual cathodes. The virtual cathode is a moving emission boundary, which is supported by the external field due to the electron flow after the virtual cathode. In turn, the plasma expansion leads to the virtual cathode migration toward the anode, additional increase in the ion concentration nearby the current potential drop, and anomalous ion acceleration. The virtual cathode depth Δφ remains unchanged during the vacuum gap delay, the initial drop of the current potential being maintained by the continuous emission.

Ecton based cathode plasma expansion

The ecton based emission is shown in Fig. 3. The boundary condition (7) with the emission specified as a pulse-periodic function is used with other constant parameters $t_{rise} = 0.1$ ns, $t_{width} = 3$ ns, $T = 5$ ns for the function $\chi(t)$. These parameters are used to model the pulsed plasma emission from the cathode such that the average emission current is on the order of magnitude close to that for the continuous plasma emission and provides the high cathode emissivity. Moreover, these parameter values are in good agreement with the experimental data [1].

In Fig. 3, the distribution of the electrostatic potential is obtained at the maximum emission current. A comparison of Figs. 2 and 3 shows that the ion and electron motion does not differ significantly. When the emission current density is maximum, the virtual cathode amplitude Δφ is –100 V. The current potential distribution and the charged particle concentration are approximately the same in both cases. In the case of the ecton emission, the average velocity of the ionic component is slightly lower, *viz*. ~2.2·10^6 cm/s, which is close to the parameters of the cathode flare plasma observed in [1]. This is due to the interval between two neighboring pulses observed during the ecton emission, when the cathode completely loses its emission capacity.

According to [9], the initial drop of the current potential nearby the emission boundary at the cathode, occurs for less than 0.1 ns. It results in the formation of the virtual cathode region, which enables the plasma expansion into the gap due to the external field. This drop of the current potential results from the basic phenomenon of the localized decay of the cathode plasma bunch on the periphery [20]. In this region, the particle concentration is by the order of magnitude lower than in the cathode region, and the condition of the plasma approximation on the periphery is not satisfied. Being lighter and thermalized particles, electrons displace from their initial state even in the absence of the external field, which leads to the formation of the negative bulk charge at the edges of the cathode plasma bunch, which is determined by the concentration n_0 [19, 20]. Thus, the initial short emission pulse (ecton) at $t = 0$ enables the cathode plasma expansion.

In both types of the plasma emission (Figs. 2, 3), the inoculating potential drop is almost an instantaneous phenomenon if we compare it with the ecton lifetime. Regardless of the plasma emission mode, this fact initiates the electron flow according to the Child–Langmuir law. During 3 to 5-ns lifetime of the first ecton, the ions moving toward the anode accelerate, and the plasma emission boundary slightly shifts to the right. The formation and motion of the virtual cathode leads to the ion acceleration both for the continuous (Fig. 2) and ecton (Fig. 3) emission at the cathode. By the moment of the gap bridging by the plasma, the ions acquire the kinetic energy of ~300 eV, although the absolute value Δφ never exceeds 100 V. Due to the momentum of the ionic plasma component, the ion motion continues for several nanoseconds between the ecton's death and birth. A further emission burst leads to another potential redistribution and plasma expansion.

The circuit current grows and the voltage in the ballast resistor drops with the plasma motion to the anode, thereby causing a gradual decrease in the anode potential. The electron flow lowers, resulting in a decrease in the virtual

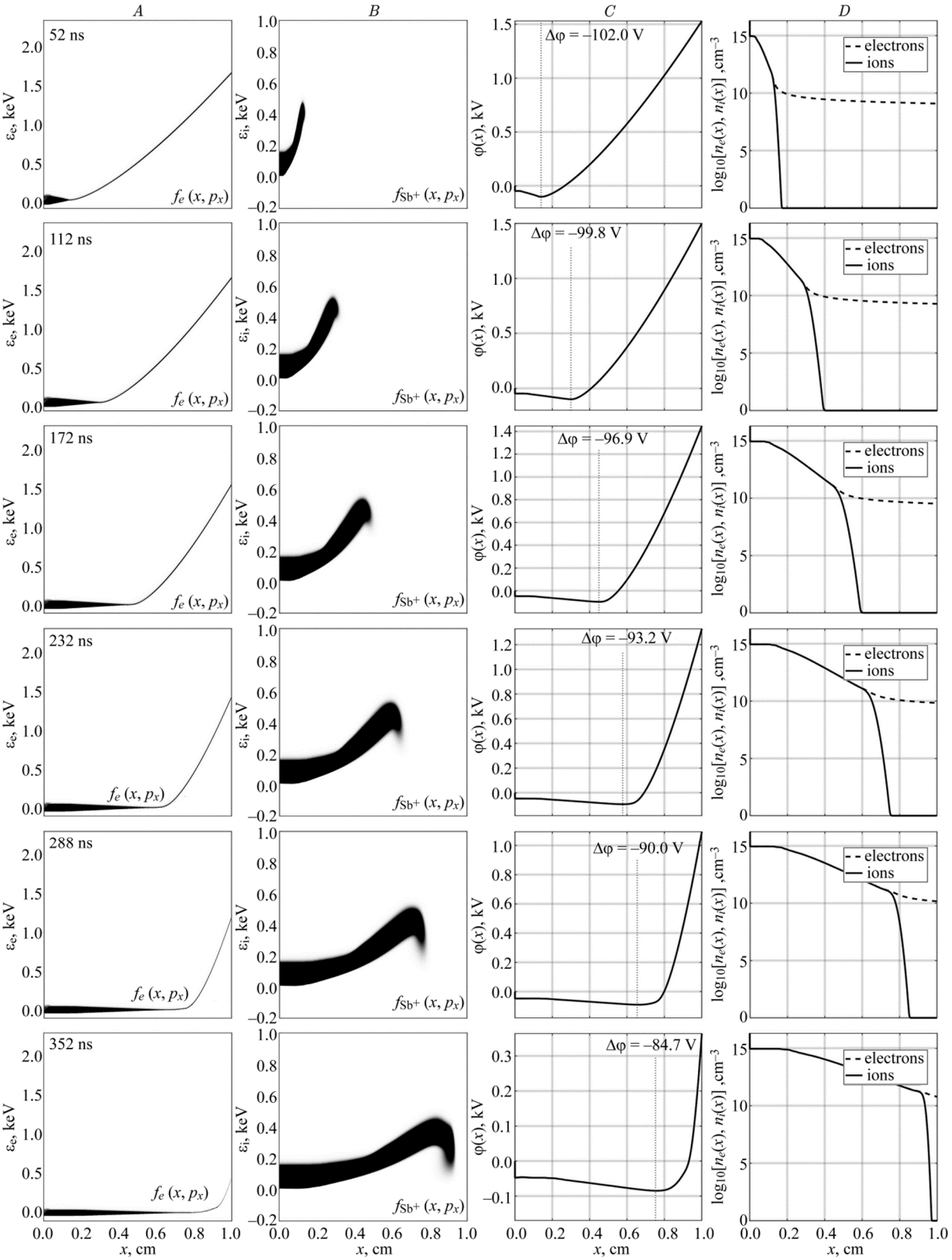

Fig. 2. Continuous plasma emission. Spatial and temporal dynamics of electron (*A*) and ion (*B*) distribution functions, electrostatic potential (*C*), and concentration of charged particles (*D*) at different time.

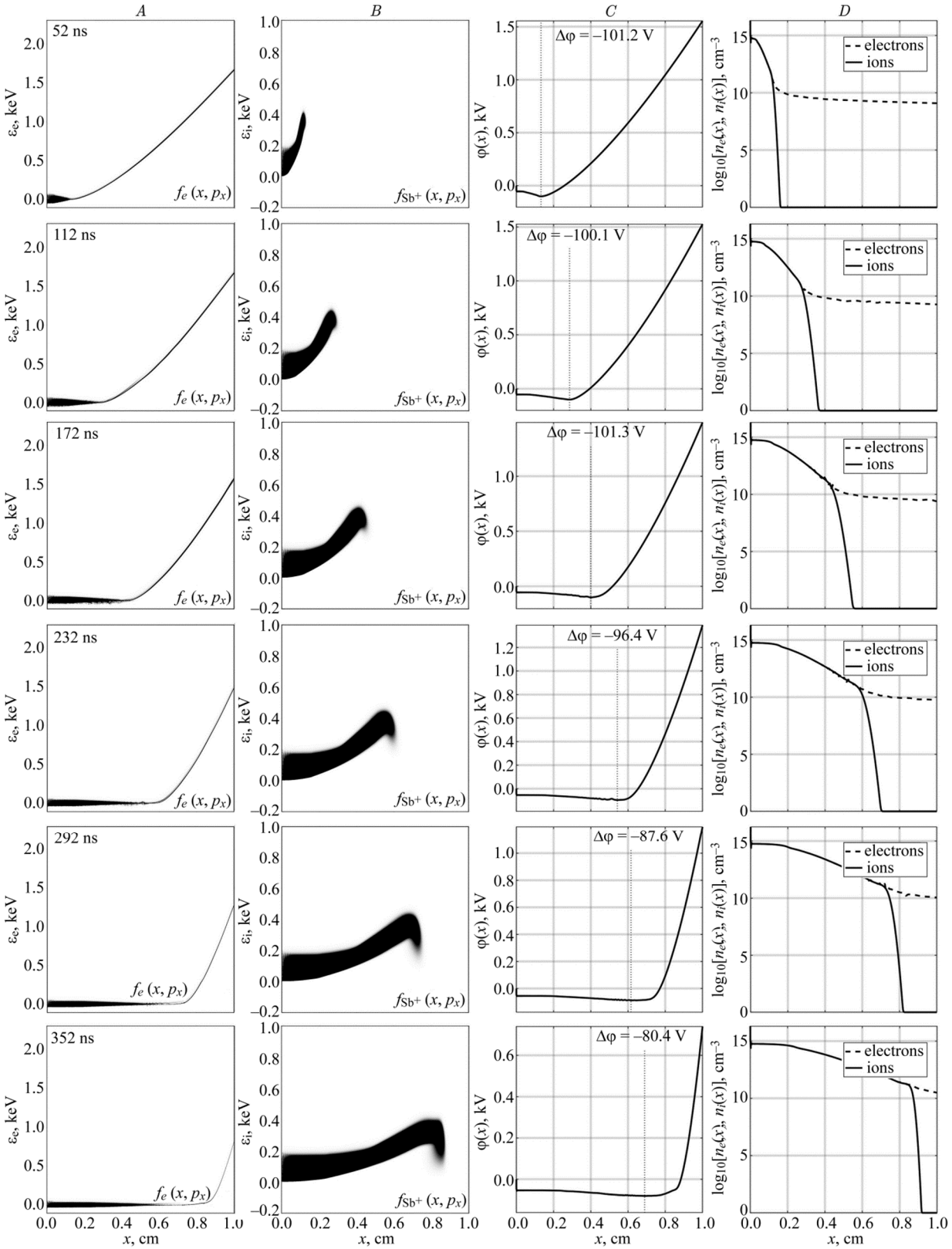

Fig. 3. Ecton based plasma emission. Spatial and temporal dynamics of electron (*A*) and ion (*B*) distribution functions, electrostatic potential (*C*), and concentration of charged particles (*D*) at different time.

cathode amplitude $\Delta\varphi$. The ions continue to accelerate and, depending on the ballast resistance and average kinetic energy gained during the motion, overcome the residual anode potential. This ion dynamics is observed for both emission modes.

Another common feature of the cathode plasma expansion, is the electron component behavior near the cathode. According to Figs. 2*a* and 3*a*, the electrons are heated near the cathode due to a return of their small part to the cathode. The expanding quasi-neutral plasma charged to the negative potential, effectively shields the cathode region, and the emission mode does not significantly modify its expansion.

Of particular interest is the instantaneous redistribution of the current potential and the bulk charge of plasma particles during its pulsed emission. What exactly happens during the so-called "dead time" (short time between emission bursts) in the absence of the emission current from the cathode? In order to answer this question, the electron distribution function and the current potential are additionally specified at $t = 50$ to 55 ns, covering one emission pulse from the cathode. In order to exclude the redistribution effect of the voltage drop between the diode and ballast resistance, we assume that the voltage source (anode potential) is ideal ($R = 0$). Other parameters of the vacuum gap, potential pulse, and $\chi(t)$ function are similar to those used above. The calculation results are presented in Fig. 4.

The emission current from the cathode begins to grow at $t = 50$ ns of the next pulse initiation. By this moment, the emission is absent for 2 ns, the electric potential distribution is similar to the current flow from the quasi-neutral plasma, the boundary of which locates near the minimum ($\Delta\varphi = -1.3$ V) of the electrostatic potential $x = 0.1$ cm.

The potential distribution considerably changes starting from $t = 50.1$ ns, when the emission current flows into the gap, to $t = 53$ ns of the emission end. The virtual cathode formation with the amplitude $\Delta\varphi = \sim 100$ V (similar to that in Figs. 2, 3) occurs at the expected point of the plasma emission boundary. It is described by a dramatic potential drop of about –50 V near the cathode and a smooth potential curve leading to the minimum at $\Delta\varphi = -100$ V. During this time, fluctuations of the bulk charge of particles (see Fig. 4) are caused by the birth of a new ecton and the emission current flow into the quasi-neutral plasma, which is under conditions of the electron flow. At $t_{width} = 3$ ns, the plasma expansion occurs due to both the accelerating electric force and inertial properties of the ionic component.

At $t = 53$ ns, the ecton dies, i.e., the plasma emission from the cathode interrupts. Therefore, already at $t = 53.1$ to 55 ns interval between pulses, the virtual cathode rapidly smooths ($t = 55$ ns, $\Delta\varphi = -3.7$ V) and the quasi-neutral plasma discharges. Afterwards, the new ecton birth provides the process continuation.

Note that during the whole process, the anode voltage is constantly high, and the electron flow continues. Moreover, it is the constant influence of the external field on the electron flow, that leads to a smooth failure of the virtual cathode during intervals between the ecton emission.

CONCLUSIONS

A comparison of numerical simulation results of the vacuum arc in the planar diode with the continuous plasma emission from the cathode and ecton based plasma emission, showed that the cathode plasma expansion was a collision-free process in the electric field.

Without loss of generality, it should be noted that the vacuum arc initiated when the emission center emitted a quasi-neutral plasma bunch, which acquired a negative bulk charge at its periphery. That led to a localized violation of the electroneutrality condition and the formation of the virtual cathode, which provided the accelerated ion flow towards the anode. The virtual cathode region became a conventional boundary of the electron beam emission, while the physical cathode was effectively shielded by the expanding plasma. Due to the potential difference applied to the diode, the gradual ion accumulation resulted in the cross-sectional motion of the virtual cathode towards the anode, which, in turn, contributed to the successive accelerated ion flow to the anode and the cathode plasma expansion.

More detailed kinetic modeling of the vacuum arc in the planar diode with the ecton emission showed the following:

– the duration of the initial current potential drop was significantly shorter than the time of the ecton nucleation. The cathode plasma expansion therefore occurred at the first ecton formation;

– the death of one ecton and time before the next ecton birth led to a temporary disappearance of the virtual cathode ($\Delta\varphi \sim 0$), but did not stop the cathode plasma expansion to the anode;

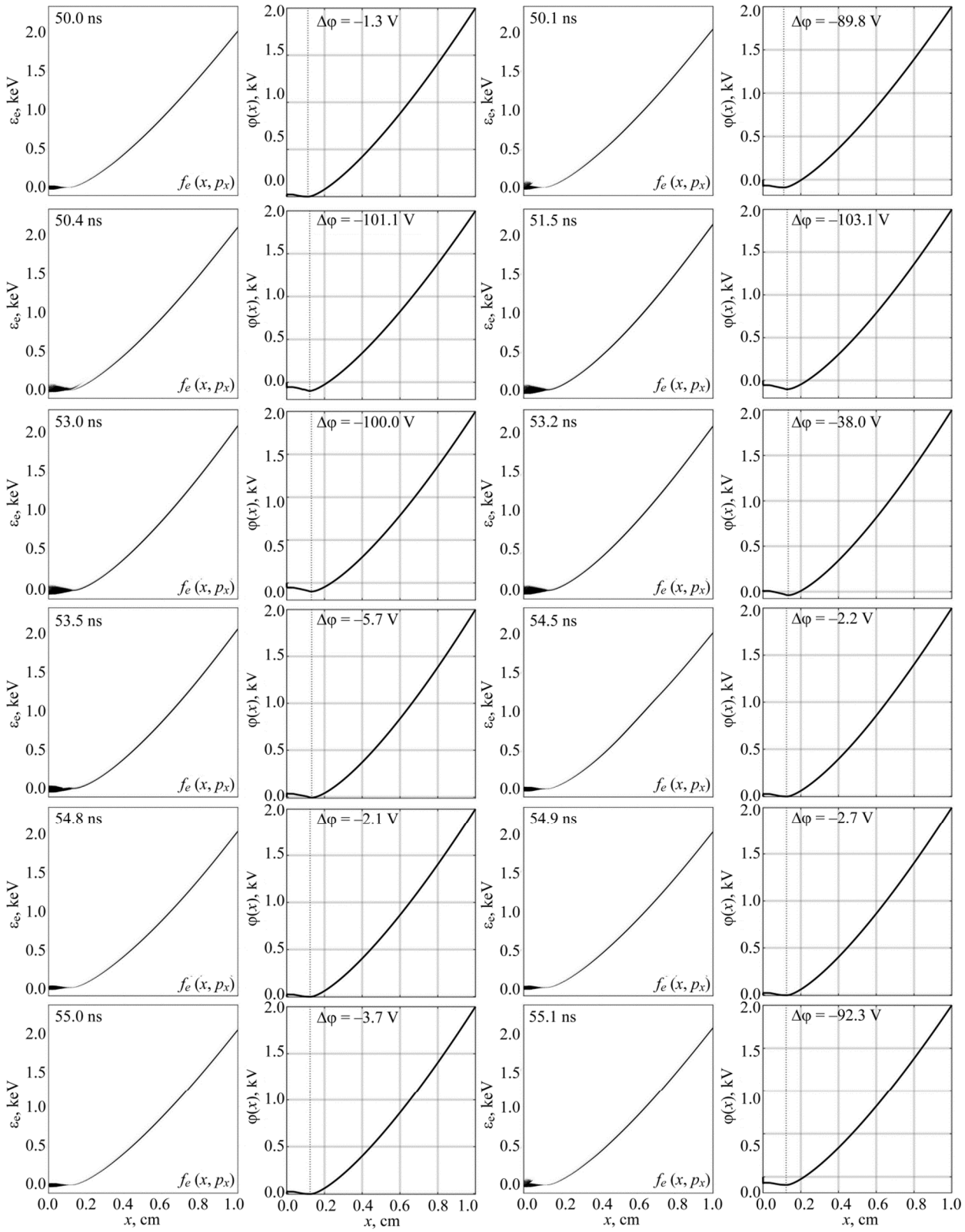

Fig. 4. Spatial and temporal dynamics of electron distribution function and electrostatic potential distribution during one (11th) cycle of the pulse-periodic plasma emission from the cathode.

– the plasma expansion between bursts of the emission current occurred at the outer emission boundary of the quasi-neutral plasma. For ions, it occurred due to the inertial properties of the ionic component and its kinetic energy acquired during the ecton lifetime (emission);

– the birth of each ecton led to the formation of a new virtual cathode at the outer emission boundary and acceleration of a new portion of the ionic component at the electrostatic potential drop.

COMPLIANCE WITH ETHICAL STANDARDS

Author contributions

Conceptualization, methodology, writing—conclusion and editing A. V. K.; methodology, computations, investigation, data analysis, writing—original draft preparation V. Yu. K.; computation, data curation, illustrations A. O. K. All authors have read and agreed to the published version of the manuscript.

Conflict of interest

The authors declare no conflict of interest.

Financial interests

The authors declare they have no financial interests.

Funding

This work was financially supported by Grant No. 23 29 00239 from the Russian Science Foundation.

Statement of the supervisory board

Authorized.

Declaration of competing interest

The authors declare no financial interests/personal relationships which may be considered as potential competing interests.

Data availability statement

The data that support the findings of this study are available from the corresponding author upon reasonable request.

REFERENCES

1. G. A. Mesyats, Explosive Electron Emission [in Russian], Fizmatlit, Moscow (2011).
2. G. Yu. Yushkov, A. S. Bugaev, I. A. Krinberg, and E. M. Oks, Doklady Phys., **46**, No. 5, 307−309 (2001).

3. E. M. Oks, K. P. Savkin, G. Y. Yushkov, *et al*., Rev. Sci. Instrum., **77**, No. 3, 03B504 (2006).
4. N. B. Volkov and A. Z. Nemirovsky, J. Phys. D, **24**, No. 5, 693–701 (1991).
5. C. Wieckert, Beiträge aus der Plasmaphysik, **27**, No. 5, 309–330 (1987).
6. E. V. Nefedtsev and A. V. Batrakov, in: Proc. 27th Int. Symp. "Discharges and Electrical Insulation in Vacuum," Suzhou, China (2016), p. 37.
7. W. D. Davis and H. C. Miller, J. Appl. Phys., No. 40, 2212 (1969).
8. A. Anders, Phys. Rev. E, **55**, No. 1, 969–981 (1997).
9. V. Kozhevnikov, A. Kozyrev, A. Kokovin, and N. Semeniuk, Energies, **14**, No. 22, 7608 (2021).
10. A. V. Kozyrev, V. Y. Kozhevnikov, N. S. Semeniuk, and A. O. Kokovin, Plasma Sources Sci. Technol., **32**, No. 10, 105010 (2023).
11. V. Y. Kozhevnikov, A. V. Kozyrev, A. O. Kokovin, and N. S. Semenyuk, Plasma Phys. Rep., **49**, No. 11, 1350–1357 (2023).
12. V. Y. Kozhevnikov, A. V. Kozyrev, V. S. Igumnov, N. S. Semenyuk, and A. O. Kokovin, Fluid Dyn., **58**, No. 6, 1148–1155 (2023).
13. A. Anders, in: Proc. 26th Int. Symp. Symp. "Discharges and Electrical Insulation in Vacuum," Mumbai, India (2014), pp. 201–204.
14. G. A. Mesyats, Cathode Phenomena in Vacuum Discharge: Breakdown, Spark and Arc [in Russian], Nauka, Moscow (2000).
15. Y. Y. Urike, in: Proc. 5th Int. Symp. Symp. "Discharges and Electrical Insulation in Vacuum," Poznan, Poland (1972), pp. 111–114.
16. J. D. Cross, B. Mazurek, and K. D. Srivastava, IEEE Electr. Insul. Mag., **18**, No. 3, 230–233 (1983).
17. G. Strang, Siam. J. Numer. Anal., **5**, No. 3, 506–517 (1968).
18. C. Cheng and G. Knorr, J. Comput. Phys., **22**, No. 3, 330–351 (1976).
19. K. Ren, M. Alam, P. P. Nielsen, M. Gussmann, and L. Rönnegård, Frontiers in Animal Science, **24**, No. 3, 1–11 (2022).
20. D. S. Dorozhkina and V. E. Semenov, Phys. Rev. Lett., **81**, No. 13, 2691–2694 (1998).